

# Biological heterogeneity of putative bladder cancer stem-like cell populations from human bladder transitional cell carcinoma samples

Angela Bentivegna,<sup>1</sup> Donatella Conconi,<sup>1</sup> Elena Panzeri,<sup>1</sup> Elena Sala,<sup>2</sup> Giorgio Bovo,<sup>3</sup> Paolo Viganò,<sup>4</sup> Silvia Brunelli,<sup>5</sup> Mario Bossi,<sup>1</sup> Giovanni Tredici,<sup>1</sup> Guido Strada<sup>4</sup> and Leda Dalpra<sup>1,2,6</sup>

<sup>1</sup>Dipartimento di Neuroscienze e Tecnologie Biomediche, Università degli Studi di Milano-Bicocca, Monza; <sup>2</sup>US Genetica Medica, <sup>3</sup>UO Anatomia patologica, Ospedale San Gerardo, Monza; <sup>4</sup>Divisione Urologia, Ospedale Bassini ICP, Milano; <sup>5</sup>Dipartimento di Medicina Sperimentale, Università degli Studi di Milano-Bicocca, Monza, Italy

(Received June 29, 2009/Revised October 15, 2009/Accepted October 16, 2009/Online publication November 30, 2009)

Transitional cell carcinoma (TCC) is the most common type of bladder cancer. Emerging evidence has suggested that the capability of a tumor to grow and propagate is dependent on a small subset of cells, the cancer stem-like cells (CSCs) or tumor initiating cells. We report on the isolation and biological characterization of putative bladder CSC populations from primary TCCs. Isolated cells were induced to proliferate in stem cell culture conditions (serum-free medium containing mitogenic growth factors). The proliferating cells formed spheroids (urospheres) and their abilities for extensive proliferation and self-renewal were assayed. Their positivity for several stem cell markers (CD133, Oct-3/4, nestin, and cytokeratins) was also assessed by immunofluorescence tests and they could have the potential to differentiate in the presence of serum. In stem cell culture conditions they gradually showed loss of proliferation, adherence to the substrate, and morphological changes, which might reflect their progressive acquisition of differentiative capacity and loss of self-renewal ability. To evaluate if effective cell selection occurred after isolation, conventional cytogenetic studies on fresh chromosome spreads immediately after isolation and after culture were carried out. In addition, a molecular cytogenetic study by UroVysion assay was carried out on paraffin-embedded tissue sections and on fresh and after culture nuclei preparations. The data collected indicated important karyotype changes and a positive selection for hypo- or near-diploid cells, losing the complexity present in fresh tumors. (*Cancer Sci* 2010; 101: 416–424)

Bladder cancer is the fifth most common tumor in the USA, accounting for 5–10% of all malignancies.<sup>(1)</sup> Histologically, more than 90% of bladder cancers are epithelial transitional cell carcinomas (TCC). Superficial TCC is heterogeneous in molecular pathogenesis and 60–90% of patients will have a tumor recurrence if treated by transurethral resection alone.<sup>(2)</sup>

The high frequency of recurrence of superficial TCC of the bladder and its heterogeneous presentation prompted us to suppose that stem cells (or cells that by mutation acquired stem peculiarities) could be involved in the development of this kind of tumor. Cancer stem cells (CSCs) constitute a rare population of undifferentiated tumorigenic cells responsible for tumor initiation, maintenance, and spreading.<sup>(3)</sup> For tumors containing a subpopulation of CSCs, there are at least two proposed mechanisms for how the CSCs could have arisen: oncogenic mutations that inactivate the constraints on normal stem cell expansion; or, in a more differentiated cell, oncogenic mutations could generate continual proliferation of cells that no longer enter a postmitotic differentiated state, thereby creating a pool of self-renewing cells in which further mutations can accumulate.<sup>(3)</sup> Current failure of cancer therapies might be due to their lower

effect on CSCs that retain their full capacity to undergo and to restore the tumor cell mass. The development of new CSC-targeted therapies is currently hindered by the lack of reliable markers for the identification of CSCs and the poor understanding of their behavior and fate determinants. CSCs have been isolated from leukemia<sup>(4)</sup> and several solid tumors.<sup>(5–8)</sup> These cells can be expanded *in vitro* as tumor spheres, and are able to reproduce the original tumor when transplanted in immunodeficient mice. The existence of CSCs has also recently been reported in human bladder cancer.<sup>(9–11)</sup>

## Materials and Methods

**Patients, tissue collection, and cell cultures.** Clinical specimens were collected between 2006 and 2008 after clinically indicated transurethral resections from 49 patients (42 males and 7 females). The age range of patients was 53–88 years (average 73 years) for males and 58–87 years (average 79.5 years) for females. Informed consent was obtained before tissue collection. All resected tissue was examined by one pathologist; staging and grading were done according to the World Health Organization Consensus Classification.<sup>(12)</sup>

Primary tumor samples were subjected to mechanical and enzymatic dissociation. Before digestion with collagenase, samples were cut up into small pieces with scissors then minced completely using sterile scalpel blades. To obtain single-cell suspensions, the resultant minced tumor pieces were mixed with collagenase H (Roche, Mannheim, Germany) 0.1% in DMEM/F12 (Invitrogen, Milano, Italy) and allowed to incubate at 37°C for 2–3 h for enzymatic dissociation. They were then passaged through needles with decreasing diameters and filtered through a 40- $\mu$ m nylon mesh. The resulting cells were cultured with epidermal growth factor and basic fibroblast growth factor (TebuBio, Rocky Hill, NJ, USA) 20 ng per mL in two culture conditions: (i) DMEM and serum-free conditions; and (ii) advanced DMEM/F12 with 0.5% FCS. Cells were seeded in 5-mL flasks at a low density ( $2 \times 10^4$  viable cells/cm<sup>2</sup>) in the absence of supplementary substrate or adhesion factors.

*In vitro* differentiation tests were carried out on isolated CSCs cultured for 1 month in the above conditions. The cells were then passaged in RPMI-1640 (Euroclone Spa, Milano, Italy) supplemented with 20% FCS but without the addition of mitogenic growth factors.

**PKH staining.** To evaluate whether urospheres showed a clonal origin, they were stained with fluorescent cell membrane dyes PKH2 and PKH26 (Sigma, Milano, Italy). Cultured cells were harvested, centrifuged, washed with  $1 \times$  PBS and divided

<sup>6</sup>To whom correspondence should be addressed.  
E-mail: leda.dalpra@unimib.it

into two groups: one was suspended with PKH2 dye (green) and the other with PKH26 (red) in the supplied diluents A and C, respectively. The labelling conditions were 20 millions/mL. After incubating the two groups of cells with their respective labels at room temperature (RT) for 3 min, the reaction was stopped by adding an equal volume of BSA 1% and medium without growth factors to remove unbound dye. The labelled cells were then centrifuged and washed in medium without growth factors. The two groups of cells were then mixed and seeded together at a concentration of 80 000 cells/mL. After 1 week of culture the cells were harvested, centrifuged, washed with 1 × PBS and placed onto slides by Cytospin at 100g for 5 min. Cells were observed and photographed with a fluorescent microscope (Leica, Mannheim, Germany).

**Immunofluorescent staining.** Cells were grown on coverslips or placed onto slides by Cytospin, fixed with 4% paraformaldehyde for 15 min followed by permeabilization with 0.6% Triton X-100 in PBS for 30 min. Cells were incubated with the primary antibody overnight at 4°C, then with the secondary fluorescent antibody for 1 h at RT. The polyclonal rabbit antihuman CD133 (1:100; Santa Cruz Biotechnology, Santa Cruz, CA, USA), recently judged suitable,<sup>(13)</sup> the monoclonal mouse antihuman Oct-3/4 (1:50; Santa Cruz Biotechnology), the monoclonal mouse antihuman cytokeratin 5, 14, 8/18 (1:50; Santa Cruz Biotechnology), the monoclonal mouse antihuman nestin (1:100; Chemicon, Temecula, CA, USA), and the monoclonal mouse antihuman nuclei (1:100; Chemicon) were applied. Alexa Fluor 488-, 546-, and 647-conjugated antimouse or Alexa Fluor 488-conjugated antirabbit (1:200; Invitrogen) were used as secondary antibodies. In negative controls the first antibody was eliminated. DAPI or propidium iodide staining for DNA was also carried out. Fluorescent cell preparations were examined using a Nikon Eclipse E600 laser scanning confocal microscope (Nikon, Melville, NY, USA).

**Immunohistochemical staining.** Formalin-fixed paraffin-embedded tissue sections were deparaffinized with xylene, rehydrated in descending concentrations of ethanol, and boiled for 30 min in citrate buffer (10 mM, pH 6.0). Endogenous peroxidase activity was suppressed with 3% H<sub>2</sub>O<sub>2</sub> for 5 min. Slides were incubated with the monoclonal mouse antihuman Oct-3/4 (1:50; Santa Cruz Biotechnology), or the monoclonal mouse antihuman cytokeratin 5, 14, 8/18 (1:50; Santa Cruz Biotechnology) for 30 min at RT then stained with an ABC staining system kit (Santa Cruz Biotechnology). In negative controls the first anti-

body was eliminated. Seminoma slides were used as positive controls for Oct-3/4.

**Cytogenetic analysis.** Following a 6-h colcemid treatment (0.1 µg/mL), cells were subjected to hypotonic treatment with 0.56% KCl for 20 min at RT then fixed with 3:1 methanol:acetic acid for 10 min. Cells were dropped onto glass slides and allowed to dry. Chromosome preparations were analyzed by QFQ banding and the karyotype described as recommended.<sup>(14)</sup>

FISH analysis on paraffin-embedded tissues, isolated interphasic nuclei, and after culture preparations was carried out using a UroVysion assay (Vysis, Wiesbaden, Germany). The hybridization, signal evaluation and counting were carried out according to the manufacturer's protocol. At least 100 cells for each preparation were scored.

All digital images were captured using a Leitz microscope (Leica DM 5000B) equipped with a charge coupled device (CCD) camera and analyzed by means of Chromowin software (Casti Imaging, Venezia, Italy).

**Transplantation of tumor cell suspensions into immunodeficient mice.** Tumor cells (100 000 or 150 000) were resuspended in 200 µL PBS and grafted under the left subcapsular renal space of 10-week-old CD1 nude female mice (Charles River Laboratories, Calco, Italy). After 8 weeks, grafts were recovered, fixed in 4% paraformaldehyde (PFA) and processed for immunohistochemistry.

## Results

**Isolation and expansion potentiality of bladder CSCs.** In this study we collected 50 primary TCCs. In Italy there is a screening program for this type of tumor, so diagnosis and surgical removal are very timely. Consequently, the size of the specimens was always very small (53% were ≤1 cm). A summary of histological results and isolation data is reported in Table 1. We were able to establish cultures from 40 cases because in 10 the tumor was of inadequate size for processing. Furthermore, for 17 samples the number of isolated cells was under 1 × 10<sup>6</sup>, making it very difficult to analyze them by FACS. In 11 cases the cultures died within 1 week.

Based on the data of published reports, we used two different culture conditions that could favor stem cell growth (see 'Materials and Methods'). For 26 samples a minority fraction of cells immediately after the isolation (24–48 h) grew into clonally derived sphere-like clusters, that we named 'urospheres'. We

**Table 1. Summary of bladder cancer sample histotypes used in this study**

| Histological diagnosis | Cited samples in the text                | Tumor size (cm) |     |   |     |   |   |   |    |
|------------------------|--|-----------------|-----|---|-----|---|---|---|----|
|                        |  | <0.5            | 0.5 | 1 | 1.5 | 2 | 3 | 4 | >4 |
| TCC LGNI<br>17 (34.7%) | 012CR08<br>039CR07<br>050CR07<br>031CR08 | 0               | 3   | 9 | 1   | 3 | 0 | 0 | 1  |
| TCC LGIN<br>2 (4.08%)  | 032CR07<br>051CR07                       | 0               | 0   | 1 | 0   | 0 | 1 | 0 | 0  |
| TCC HGNI<br>3 (6.12%)  | 016CR06<br>034CR07                       | 0               | 0   | 1 | 1   | 0 | 0 | 0 | 1  |
| TCC HGIN<br>21 (42.8%) | 019CR06<br>037CR07<br>045CR07            | 0               | 1   | 5 | 1   | 5 | 5 | 1 | 3  |
| LMP<br>5 (10.2%)       | —  | 2               | 1   | 2 | 0   | 0 | 0 | 0 | 0  |
| CIS<br>1 (2.05%)       | —  | 0               | 1   | 0 | 0   | 0 | 0 | 0 | 0  |

—, indicates no samples cited. CIS, carcinoma *in situ*; HGIN, high grade infiltrating; HGNI, high grade non-infiltrating; LGIN, low grade infiltrating; LGNI, low grade non-infiltrating; LMP, low malignant potential; TCC, transitional cell carcinoma.

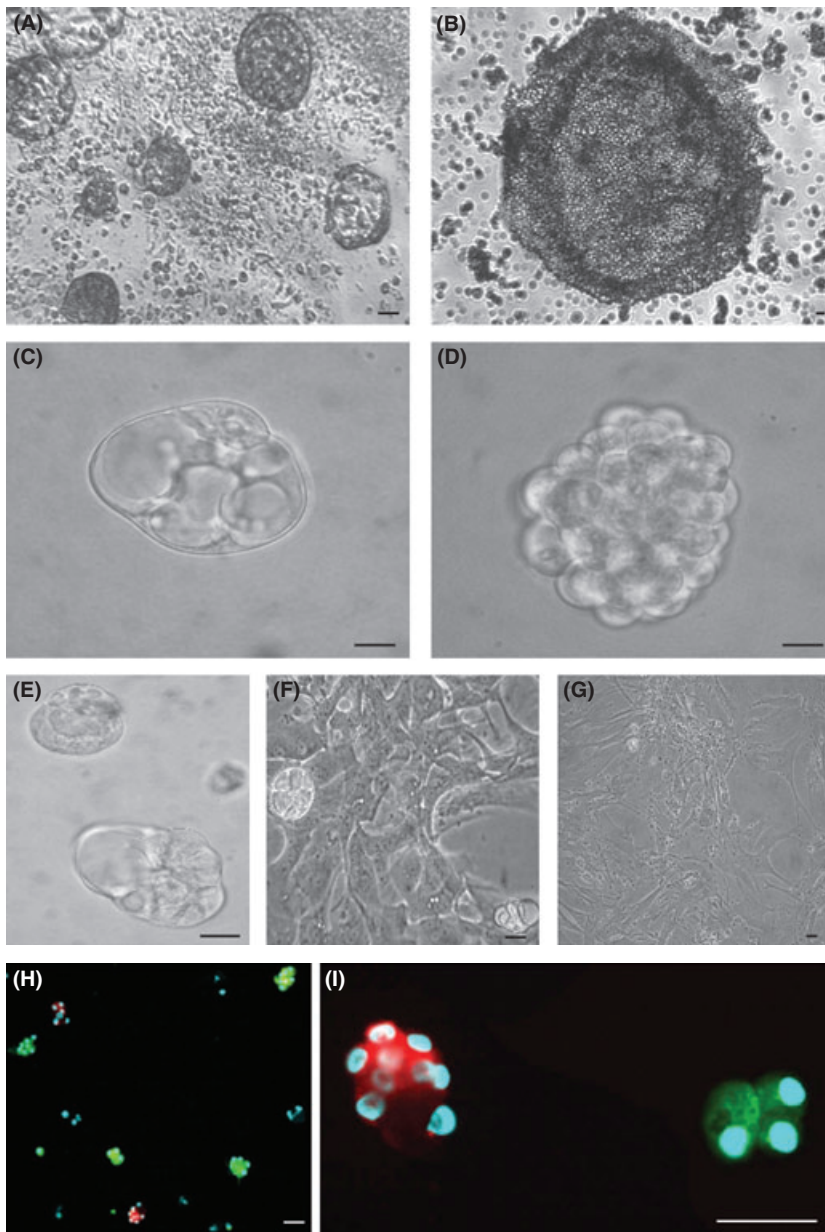


**Fig. 1.** Epidermal growth factor (EGF)/basic fibroblast growth factor (bFGF) induced proliferation of cancer stem-like cells from human transitional cell carcinomas of the bladder. (A,B) Cell culture derived from 016CR06 in DMEM, in the presence of EGF/bFGF and serum-free conditions: urospheres after 24 h (A) and sheet-like colonies after 1 week of culture (B). (C,D) Urospheres after 2 weeks of culture in DMEM/F12 medium, in the presence of EGF/bFGF and 1% FCS. (C) Vacuolated urospheres (from 034CR07); (D) non-vacuolated urospheres (from 039CR07). (E–G) Urospheres cultured in the same conditions as (C,D), 1 week (E), 1 month (F), and 2 months (G) after isolation from 034CR07. Morphological changes occurred in the cells and they became able to adhere to the substrate; moreover, a gradual decrease of mitotic activity was observed. (H,I) Double fluorescence images on day 7 after *in vitro* staining with PKH2 (green) and PKH26 (red) in 039CR07 urospheres, indicating their clonal origin. The nuclei were counterstained with DAPI (blue). Scale lines: 5  $\mu\text{m}$  (A,C–G); 10  $\mu\text{m}$  (B).

observed that in the first culture system (DMEM and serum-free condition), these spheres disappeared after 1 week of culture, then they were replaced by sheet-like colonies that remained for approximately 3 months in culture (Fig. 1A,B). The morphology of these sheet-like colonies were reminiscent of those of multipotent progenitors in the embryonic mouse kidney.<sup>(15)</sup> In contrast, in the second culture system (DMEM/F12 and FCS), we observed that 60% of samples generated vacuolated spheres. In approximately 40% of samples the spheres were mixed, vacuolated, and non-vacuolated (Fig. 1C,D). In these culture conditions, the isolated cells were maintained and expanded from 1 week to 5 months, with an average of 90 days *in vitro*, but the cultured cells gradually showed loss of proliferation, adherence to the substrate, and morphological changes (Fig. 1E–G).

Furthermore, we applied the techniques to functionally characterize the tumor cell populations.<sup>(16)</sup> We assessed the capabilities for long-term proliferation, self-renewal, and clonal origin of urospheres by subculturing, limiting dilution, and PKH staining. The self-renewing capacity was assessed by dissociation of the primary tumor spheres and plating the resulting cells

at clonal density: only a minority of them (approximately 2%) formed secondary spheres, although with a gradual decrease, accordingly to Reynolds data.<sup>(17)</sup> Then the self-renewing capacity was assessed by dissociation of the primary tumor spheres and plating the resulting cells at a dilution of 1 cell/well. In the limiting dilution assay the direct observation of the clone formation starting from an individual cell showed that only a small percentage of urosphere-derived cells (<5%) will generate secondary spheres (data not shown).

Finally, we assessed the clonal origin of urospheres by PKH staining.<sup>(18)</sup> Spheres were mechanically dissociated to single cells then one-half of them was stained with PKH2 and the remaining with PKH26. The stained cells were plated together and observed under a fluorescent microscope after 1 week of culture. The single cells generated urospheres that did not contain at the same time green and red cells, indicating the clonal origin of urospheres (Fig. 1H,I).

**Isolated CSCs positive for stem cell markers.** We tested the immunoreactivity of CD133 as recent findings pointed to it as representing a marker of tumor-initiating cells in human

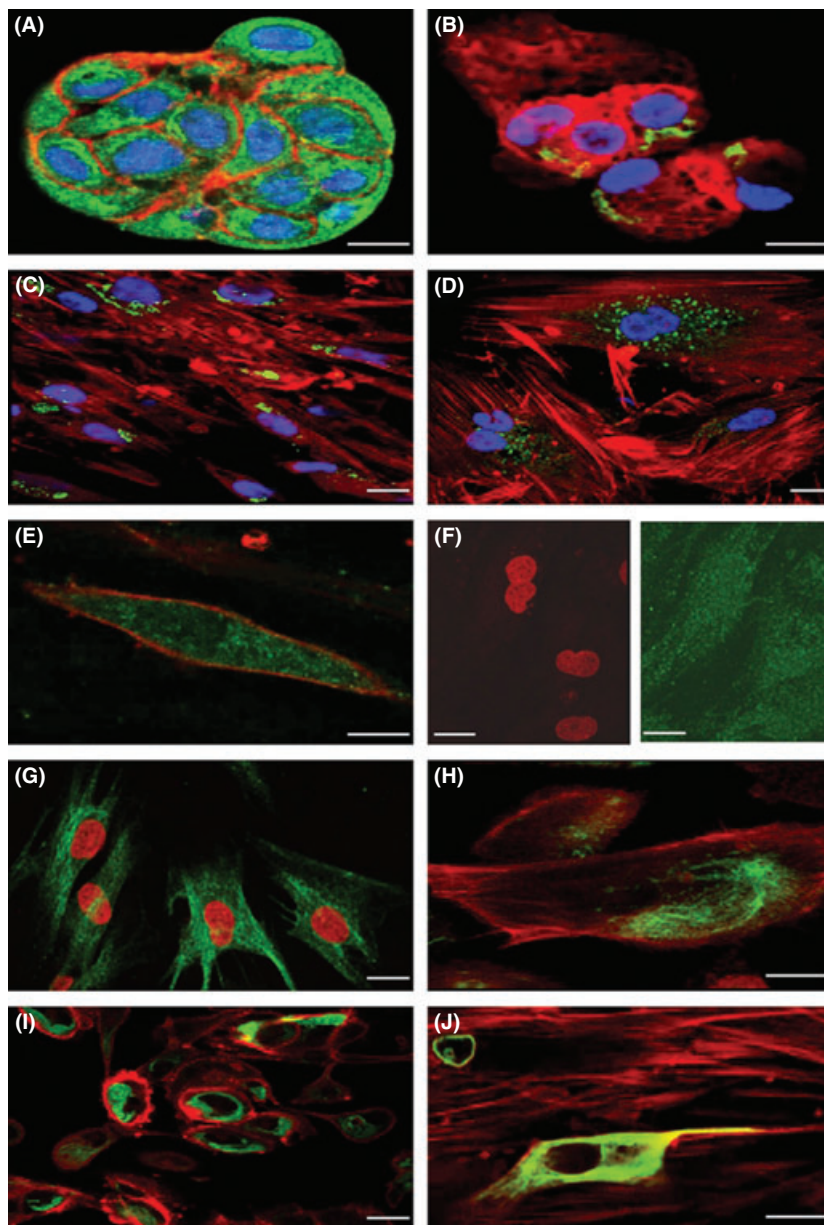


**Fig. 2.** Selected images of immunofluorescence analysis on cultured cells isolated from transitional cell carcinoma samples. (A–D) CD133 expression (green) in non-vacuolated (A, 039CR07) and vacuolated (B, 051CR07) spheres, and in adherent cells derived from urospheres of a 034CR07 sample (C,D). (E,F) Oct-4 expression (green) in adherent cells derived from urospheres of a 034CR07 sample. Note the nuclear but also cytoplasmic localization of Oct-4. (G) Nestin expression (green) in adherent cells derived from urospheres of a 012CR08 sample. (H,I) Expression of CK5 (H, green) and CK14 (I, green) in adherent cells derived from urospheres of a 050CR07 sample. (J) Expression of CK8/18 (green) in adherent cells derived from urospheres of a 034CR07 sample. Anti-actin (red) in (A–D) and (H–J); anti-nuclei (blue) antibodies in (A–D); nuclei in red (PI) in (F,G). Scale lines: 5  $\mu$ m.

cancer.<sup>(19)</sup> CD133 showed a widespread positivity in non-vacuolated spheres (Fig. 2A), but is localized and confined to the membrane area in vacuolated spheres (Fig. 2B), according to expression data for epithelial cells.<sup>(20)</sup> To assess the antigenic properties of the adherent cells, we carried out indirect immunofluorescent staining for the embryonic stem cell marker Oct-3/4 and for early progenitor cell marker nestin, in addition to CD133, and finally for cytokeratins as specific epithelial markers. Cells resulted immunoreactive for all the markers used. In particular, almost 100% of adherent cells were immunoreactive for CD133 and Oct-4, and this positivity was assessed at different times during culture (Fig. 2C–F). One hundred percent of cells were positive for nestin, with 5–10% for cytokeratins 5, 14, and 8/18 (Fig. 2G–J). These findings were reproduced in three independent cultures from three different samples of different histotype.

#### Isolated CSCs derived from subpopulations of originary tumor.

In order to evaluate a possible correlation between the heterogeneous characteristics observed in tumors *in vivo* and the heterogeneity evidenced in the isolated tumor cells with stem cell

properties *in vitro*, we checked the positivity of Oct-3/4 and cytokeratins on paraffin-embedded tumor sections (see Supporting Information, Figs S1, S2; Table S1 for quantitative data). The positivity for Oct3/4 was spread throughout the tumor section without any specific localization (Fig. S1A–C), with ~50% of positive cells, reflecting the cell heterogeneity of histological data. Conversely, immunohistochemical analysis with cytokeratins evidenced a precise and, for the most part, mutually exclusive localization of the positivity. In particular, CK5 was restricted almost exclusively to the germinative layer. CK8 was more widespread, although it showed more positivity in the luminal area of the section (see Fig. S2). The results were confirmed in at least three independent tumors of different histotype.

**Differentiation potential of isolated CSCs.** The capability to differentiate is another important feature of CSCs.<sup>(21)</sup> Cells isolated from a 012CR08 sample (see Table 1) were cultured for 1 month in serum-free conditions with epidermal growth factor and basic fibroblast growth factor (Fig. 3A–C). Then we established a parallel culture in RPMI-1640 supplemented with

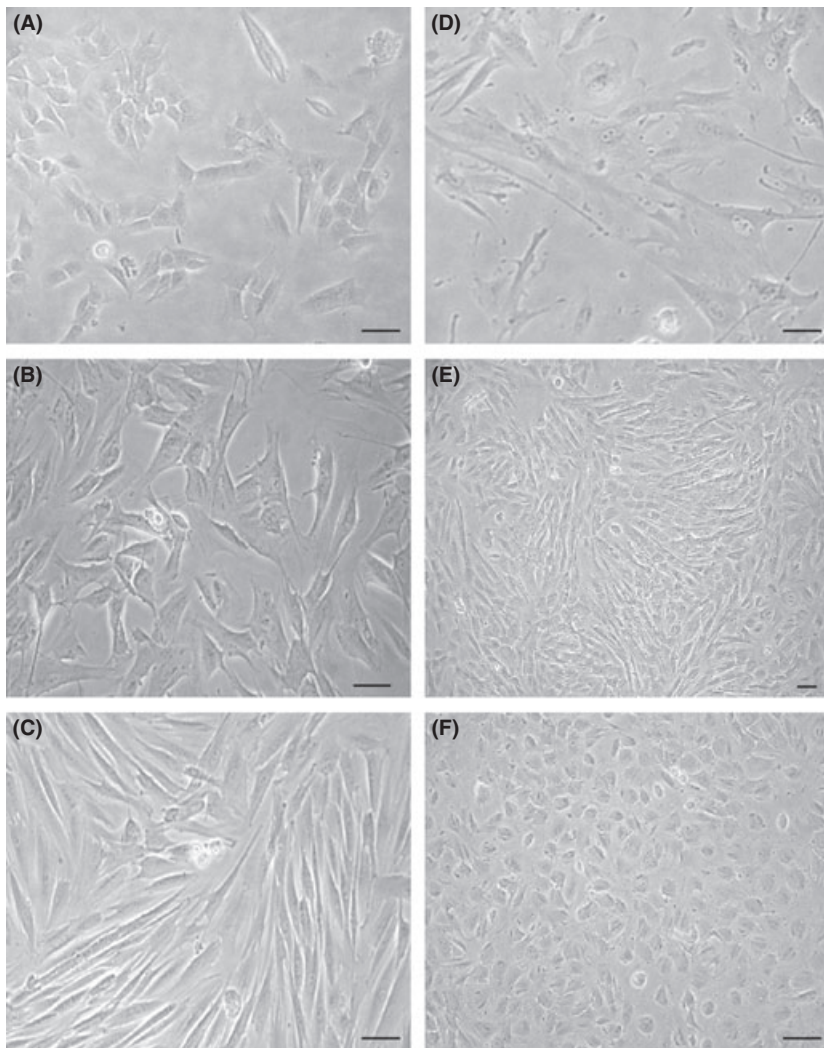


**Fig. 3.** Differentiation induction of cancer stem-like cells isolated from sample 012CR08. After 1 month in DMEM/F12 plus epidermal growth factor/basic fibroblast growth factor and serum-free conditions, the cells were passaged in the same culture conditions (A–C), or in RPMI-1640 supplemented with 20% FCS without epidermal growth factor/basic fibroblast growth factor (D–F). Note the morphology heterogeneity of cells in different areas of the same culture. The images were recorded at time 0 (A,D) and after 7 days of culture in both conditions (B,C,E,F). Scale lines: 10  $\mu$ m.

20% FCS but without mitogenic growth factors (see ‘Materials and Methods’ and Fig. 3D–F). After 1 week we observed fibroblast-like cells and a wide morphological heterogeneity in both culture conditions (Fig. 3B–F), but in RPMI-1640 we also noted the appearance of a monolayer of growing cells resembling a paved epithelium with an apparent recovery of the contact inhibition. Immunofluorescence analysis for Oct-3/4, CD133, and nestin showed a decreased percentage of cells expressing Oct-3/4 and CD133 (85% and 55%, respectively) compared to the cells of the same sample cultured in DMEM/F12 conditions. Nestin expression was found in 100% of cells in both cultures (Fig. 4A–F). In paraffin-embedded tumor sections of the sample, we also tested for the presence and localization of nestin-expressing cells, and we located them in confined areas (Fig. 4G,H). These findings were reproduced in at least three independent cultures from three different samples of different histotype.

**Cytogenetic characterization of isolated CSCs.** In order to evaluate if an effective cell selection has occurred after the isolation we carried out conventional cytogenetic analysis on fresh TCC samples and on cultured CSCs (Fig. 5). Evidence for general chromatin instability and degeneration was observed in all fresh samples and many different numerical and structural aberrations, especially Y chromosome involvement (75% out of all abnormalities observed), were detected, showing a very high karyotype complexity, nearly impossible to analyze

(Fig. 5A–E). In addition, we observed more hyperdiploid cells (82.8%) in high grade TCC, and hypodiploid cells in low grade TCC (77.3%). Cytogenetic analysis on preparations after culture indicated a general decrease of complexity with decrease/loss of complex rearrangements and chromatin instability absence; furthermore, a negative selection against the hyperdiploid cells was shown, especially in high grade TCC (Fig. 5F).

Finally, a molecular cytogenetic study using UroVysion assay on paraffin-embedded tissue sections and on fresh and after culture nuclei preparations, evidenced a significant heterogeneity also among tumors with the same histotype (Fig. 5G–I and Table S2; Fig. S3). Even if the number of samples is small, the differences in the number of signals recorded before and after culture, for each sample and for each type of event (loss [number of signals/cell <2], disomy [number of signals/cell =2], or gain [number of signals/cell >2]) a cell selection during *in vitro* culture can be assumed.

**Tumorigenicity of isolated CSCs.** To investigate the tumorigenic potential of isolated CSCs, 100 000 or 150 000 cells from two samples of low grade non-infiltrating TCC (012CR08 and 031CR08) and a high grade infiltrating TCC (019CR09) were orthotopically injected in CD-1 nude mice as described in ‘Materials and Methods’. Two months after the graft there were no visible signs of new tumours in any of the immunocompromised transplanted mice.

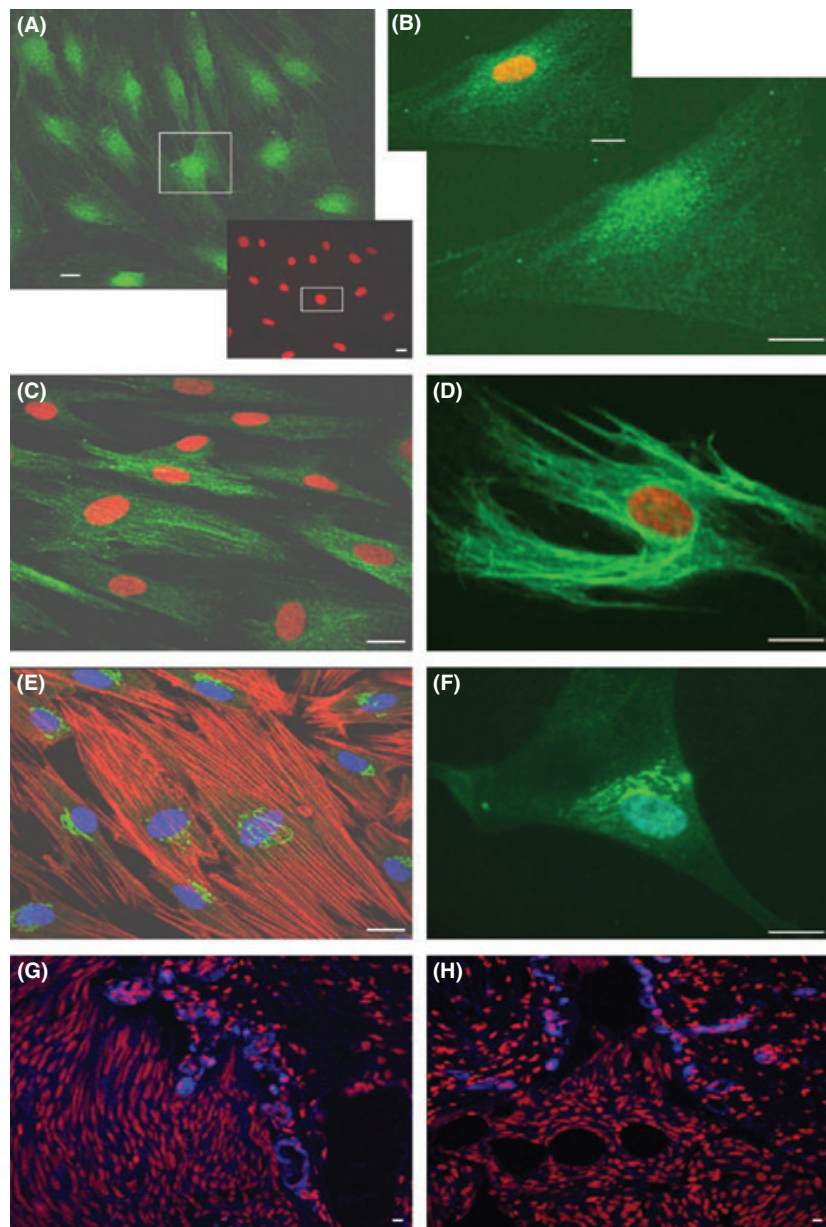


**Fig. 4.** Immunofluorescence staining in cancer stem-like cells isolated from sample 012CR08 after differentiation induction. The experiments were carried out after 1 week in DMEM/F12 plus epidermal growth factor/basic fibroblast growth factor and serum-free conditions (A,C,E) or in RPMI-1640 supplemented with 20% FCS without epidermal growth factor/basic fibroblast growth factor (B,D,F). Expression of Oct-4 (A,B), nestin (C,D), and CD133 (E,F) shown in green. Nestin expression (blue) on paraffin-embedded tumor sections of the same sample (G,H). Nuclei in red (A–D, G–H) or blue (E–F); anti-actin in red (E). Scale lines: 5  $\mu$ m.

## Discussion

In this multidisciplinary study we report on the biological-cytogenetic characterization of putative bladder CSC populations isolated from human primary TCCs (for a summary of collected data, see Table S3 in Supporting Information). Because the samples had such small dimensions we had to choose the most appropriate experiment for each. We used two different culture conditions to expand the isolated cells and we observed urosphere formation in both cases within 24–48 h. However cells only in the second system (DMEM/F12 and FCS), seemed to be expanded and maintained. In these conditions, the spheres had two different morphologies with no apparent histological grading correlation. Our preliminary results on the clonal origin, self-renewal, and long-term proliferation abilities of urospheres converged to confirm the existence of cancer cells showing stem features in human bladder TCCs, in agreement with recent reports.<sup>(9–11)</sup> Our data converged on the extreme heterogeneity of these cells, as reported by Chan *et al.*,<sup>(11)</sup> but we also showed how they can change their biological characteristics, at least

*in vitro*. Indeed, the cultured cells gradually showed loss of proliferation, adherence to the substrate, and morphological changes that might reflect their progressive enrichment in cells that could have acquired differentiative capacity and loss of self-renewal ability. The adherent cells derived from urospheres were a heterogeneous population with a majority of Oct-3/4<sup>+</sup>, CD133<sup>+</sup>, and nestin<sup>+</sup> progenitor cells, and a minority of cells positive for cytokeratins, that could be considered already programmed to differentiate. Therefore, our data seem to support the model recently proposed by Gupta *et al.* on the possible existence of plasticity between stem cells and their committed derivatives.<sup>(22)</sup> As suggested by the authors, greater phenotypic plasticity might exist in tumor cell populations than is conventionally thought, and such plasticity suggests that a dynamic equilibrium could exist between CSCs and non-CSCs within tumors. Moreover, this equilibrium may be shifted in one direction or another by contextual signals within the tumor, or in the culture systems. Therefore, the cancer stem cell model could be modified and merged with the clonal evolution model, where the intrinsic differences between tumorigenic and non-tumorigenic

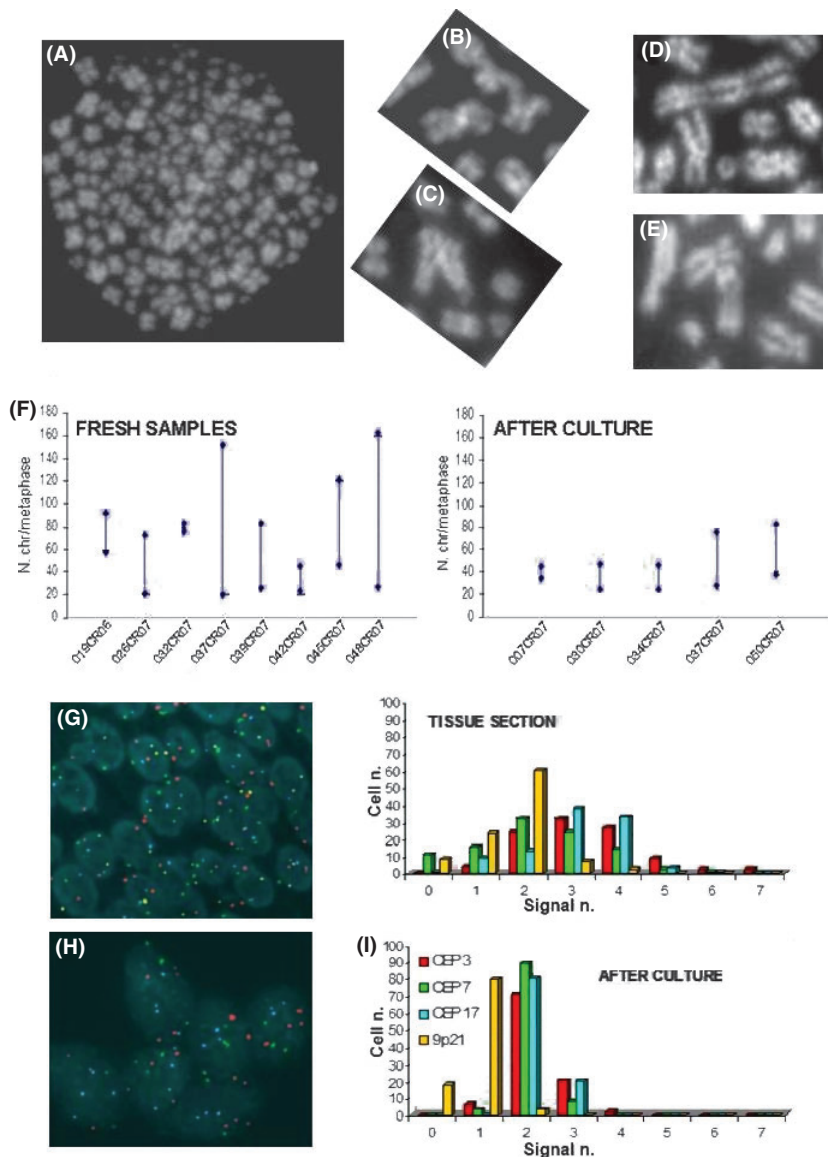


**Fig. 5.** Karyotype instability of isolated cancer stem-like cells. (A–E) Selected images of QFQ banded metaphases from cases 037CR07 (A) and 019CR06 (B, C, particulars of metaphases). Particulars of chromosomal rearrangements of chromosome 1 in 032CR07 (D) and chromosome Y aberrations in 045CR07 (E). (F) Chromosome counting results of eight fresh chromosome preparations and five after culture. A positive selection for hypo- or near-diploid cells after culture has been suggested, as evidenced by sample 037CR07, the only case in which it was possible to analyze metaphases in both preparations. (G, H) Two UroVysion FISH test examples, on a paraffin-embedded tissue section (G) and on a preparation after culture (H). (I) UroVysion FISH signals distributions versus cell numbers to identify the alterations selected by the culture conditions for sample 039CR07.

cells, instead of being stable and epigenetic, could be unstable, epigenetic, or genetic.<sup>(2,3)</sup>

To our knowledge, this is the first cytogenetic study carried out on fresh chromosome preparations and, when possible, after different times of culture, in order to evaluate the differences and possible clonal selection induced by *in vitro* conditions. Our protocol showed a positive selection for hypo- or near-diploid cells, as indicated by the general decrease of hyperdiploid cells after culture (Fig. 5F). As the number of cell, due to the small dimensions of the tumors, were not enough to carry out high-resolution comparative genomic hybridization (CGH)-array, we applied the UroVysion assay on paraffin-embedded tissue sections and nuclei samples after culture (Fig. 5G, H). This assay is designed to detect aneuploidy of chromosomes 3, 7, and 17, and the loss of the 9p21 locus on chromosome 9, and is currently used in the surveillance of patients with bladder carcinoma.<sup>(24,25)</sup> Although there are only small numbers of samples to draw conclusions, by comparing tissue and after-culture data, we observed a great heterogeneity among samples with the same histotype. Many studies have indicated that different populations of CSCs reside within the same tumor, bearing quite diverse tumorigenic potential and distinct genetic anomalies.<sup>(11,26–29)</sup>

Thus, we hypothesized that the isolated CSCs were a heterogeneous population also for cytogenetic abnormalities and the aneuploidies detected by the UroVysion assay could be later and more stable events of tumor progression. Incorporating the concept expressed by Ali and Sjöblom,<sup>30</sup> we could assume that our cells represented precancerous stages of the tumor with a heterogeneous presence of passenger mutations that, thanks to a positive selective pressure, could favour the onset of driver mutations, capable of contributing to disease progression. Once again there emerged the importance of the microenvironment for the selection of cells give rise to. Similarly, we could argue on the inability so far recorded by these cells to induce xenograft tumors *in vivo*. In this context it is necessary to remember that it has been amply established that whichever immunocompromised model was used there can be a wide variability in results of xenotransplantation, using the same number of cells derived from the same tumor;<sup>(31)</sup> see also the review by Shackleton *et al.*<sup>(23)</sup> In the recently published work of Chan *et al.*,<sup>(11)</sup> highly immunocompromised NOD/SCID mice were used, lacking T, B, and NK cells (RAG2<sup>-</sup>/γc<sup>-</sup> mice). Five of 14 tumors were successfully engrafted (four of which were high grade infiltrating tumors) after a latency of 3 months, with no obvious correla-

tions with their immunophenotype.<sup>(11)</sup> In comparison, we used CD-1 nude mice, lacking only T cells, and one low grade non-infiltrating and one high grade infiltrating tumor, with a latency of 2 months.

As previous reports have indicated a long latency required by cancer cells to induce tumors (3–6 months for glioblastomas,<sup>(26,32)</sup> 8 months for melanomas<sup>(31)</sup>), and Shackleton *et al.*<sup>(23)</sup> pointed out the extreme variability of such assays, our xenotransplantation experiments could be considered inconclusive. However, we could argue that the aggressiveness of the injected cells is very low, and in fact bladder cancer occurs mainly in older people, since it is an old-onset cancer.

In conclusion, in this study we report on the isolation and preliminary characterization of putative bladder CSC populations

from primary TCCs. Although there does not appear to be any obvious correlation with the histotype degree, further molecular and functional studies on a larger number of samples might provide valuable information of such a putative CSC population, to be exploited in the clinical setting and therefore be the target of future therapies.

## Acknowledgments

The authors thank Dr. V. Rodriguez Menendez for confocal microscopy and Dr. L. Riva for immunohistochemical analysis on paraffin-embedded sections. This work was supported by the Monza and Brianza Foundation, and the Gianluca Strada Association for research and treatment of urological cancer.

## References

- Mueller CM, Caporaso N, Greene MH. Familial and genetic risk of transitional cell carcinoma of the urinary tract. *Urol Oncol* 2008; **26**: 451–64.
- Pasin E, Josephson DY, Mitra AP, Cote RJ, Stein JP. Superficial bladder cancer: an update on etiology, molecular development, classification, and natural history. *Rev Urol* 2008; **10**: 31–43.
- Pardal R, Clarke MF, Morrison SJ. Applying the principles of stem-cell biology to cancer. *Nat Rev Cancer* 2003; **3**: 895–902.
- Bonnet D, Dick JE. Human acute myeloid leukemia is organized as a hierarchy that originates from a primitive hematopoietic cell. *Nat Med* 1997; **3**: 730–7.
- Al-Hajj M, Wicha MS, Benito-Hernandez A, Morrison SJ, Clarke MF. Prospective identification of tumorigenic breast cancer cells. *Proc Natl Acad Sci USA* 2003; **100**: 3983–8.
- Al-Hajj M, Wicha MS, Benito-Hernandez A, Morrison SJ, Clarke MF. Identification of human brain tumor initiating cells. *Nature* 2004; **432**: 396–401.
- O'Brien CA, Pollett A, Gallinger S, Dick JE. A human colon cancer cell capable of initiating tumor growth in immunodeficient mice. *Nature* 2007; **445**: 106–10.
- Ricci-Vitiani L, Lombardi DG, Pilozzi E *et al.* Identification and expansion of human colon-cancer-initiating cells. *Nature* 2007; **445**: 111–5.
- Oates JE, Grey BR, Addla SK *et al.* Hoechst 33342 side population identification is a conserved and unified mechanism in urological cancers. *Stem Cells Dev* 2009; doi:10.1089/scd.2008.0302.
- She JJ, Zhang PG, Wang ZM *et al.* Identification of side population cells from bladder cancer cells by DyeCycle Violet staining. *Cancer Biol Ther* 2008; **7**: 1663–8.
- Chan KS, Espinosa I, Chao M *et al.* Identification, molecular characterization, clinical prognosis, and therapeutic targeting of human bladder tumor-initiating cells. *PNAS* 2009; **106**: 14016–21.
- Epstein JI, Amin MB, Reuter VR, Mostofi FK. The World Health Organization/International Society of Urological Pathology consensus classification of urothelial (transitional cell) neoplasms of the urinary bladder. Bladder Consensus Conference Committee. *Am J Surg Pathol* 1998; **22**: 1435–48.
- Bidlingmaier S, Zhu X, Liu B. The utility and limitations of glycosylated human CD133 epitopes in defining cancer stem cells. *J Mol Med* 2008; **86**: 1025–32.
- Shaffer LG, Tommerup N. *ISCN 2005: An International System for Human Cytogenetic Nomenclature*. New York: Karger, 2005.
- Osafune K, Takasato M, Kispert A, Asashima M, Nishinakamura R. Identification of multipotent progenitors in the embryonic mouse kidney by a novel colony-forming assay. *Development* 2006; **133**: 151–61.
- Rietze RL, Reynolds BA. Neural stem cell isolation and characterization. *Methods Enzymol* 2006; **419**: 3–23.
- Reynolds BA, Rietze RL. Neural stem cells and neurospheres – re-evaluating the relationship. *Nat Methods* 2005; **2**: 333–6.
- Hosaka M, Hatori M, Smith R, Kokubun S. Giant cell formation through fusion of cells derived from a human giant cell tumor of tendon sheath. *J Orthop Sci* 2004; **9**: 581–4.
- Mizrak D, Brittan M, Alison MR. CD133: molecule of the moment. *J Pathol* 2008; **214**: 3–9.
- Corbeil D, Röper K, Hellwig A *et al.* The human AC133 hematopoietic stem cell antigen is also expressed in epithelial cells and targeted to plasma membrane protrusions. *J Biol Chem* 2000; **275**: 5512–20.
- Mackenzie IC. Stem cell properties and epithelial malignancies. *Eur J Cancer* 2006; **42**: 1204–12.
- Gupta PB, Chaffer CL, Weinberg RA. Cancer stem cells: mirage or reality? *Nat Med* 2009; **15**: 1010–2.
- Shackleton M, Quintana E, Fearon ER, Morrison SJ. Heterogeneity in cancer: cancer stem cells versus clonal evolution. *Cell* 2009; **138**: 822–9.
- Bergman J, Reznicek RC, Rajfer J. Surveillance of patients with bladder carcinoma using fluorescent in-situ hybridization on bladder washings. *BJU Int* 2008; **101**: 26–9.
- Steiner H, Bergmeister M, Verdorfer I *et al.* Early results of bladder-cancer screening in a high-risk population of heavy smokers. *BJU Int* 2008; **102**: 291–6.
- Piccirillo SGM, Combi R, Cajola L *et al.* Distinct pools of cancer stem-like cells coexist within human glioblastomas and display different tumorigenicity and independent genomic evolution. *Oncogene* 2009; **28**: 1807–11.
- Botchkina IL, Rowehl RA, Rivadeneira DE *et al.* Phenotypic subpopulations of metastatic colon cancer stem cells: genomic analysis. *Cancer Genomics Proteomics* 2009; **6**: 19–29.
- Beier D, Hau P, Proescholdt M *et al.* CD133(+) and CD133(-) glioblastoma-derived cancer stem cells show differential growth characteristics and molecular profiles. *Cancer Res* 2007; **67**: 4010–5.
- Günther HS, Schmidt NO, Phillips HS *et al.* Glioblastoma-derived stem cell-enriched cultures form distinct subgroups according to molecular and phenotypic criteria. *Oncogene* 2008; **27**: 2897–909.
- Ali MA, Sjöblom T. Molecular pathways in tumor progression: from discovery to functional understanding. *Mol Biosyst* 2009; **5**: 902–8.
- Quintana E, Shackleton M, Sabel MS *et al.* Efficient tumour formation by single human melanoma cells. *Nature* 2008; **456**: 593–8.
- Griffero F, Daga A, Marubbi D *et al.* Different response of human glioma tumor-initiating cells to epidermal growth factor receptor kinase inhibitors. *J Biol Chem* 2009; **284**: 7138–48.



## Supporting Information

Additional Supporting Information may be found in the online version of this article:

**Table S1.** Quantitative data of immunostaining (Immunohistochemistry).

**Table S2.** UroVysion FISH results on transitional cell carcinoma paraffin-embedded tissue sections and on cultured cancer stem-like cells from the same sample.

**Table S3.** Data summary of this study.

**Fig. S1.** Oct-4 protein expression on paraffin embedded tumor sections. (A–C) Patient 050CR07: note the random spatial distribution of positive nuclei. (D) Atypical ectopic localization of Oct-4 in a tumor section of patient 039CR07 otherwise negative for this marker. The inserts show: an enlargement of the positive nucleus (bottom left); an Oct-4 positive cell (top right) isolated from the same tumor (85% of cultured cells were positive). (E) Oct-4 expression on tumor section of patient 034CR07. (F) Oct-4 expression in human seminoma (as positive control for Oct4). Scale lines: 10  $\mu$ m.

**Fig. S2.** Differential expression of cytokeratins in two samples of transitional cell carcinoma with different histological grade. (A,B) Expression of CK5 (A) and CK8 (B) in two consecutive sections of a high grade non-infiltrating tumor (034CR07). Note the restricted positive but mutually exclusive area for both markers. (C,D) Expression of CK5 (C) and CK8 (D) on low grade non-infiltrating tumor sections (039CR07). Scale lines: 5  $\mu$ m.

**Fig. S3.** Graphic summary of UroVysion FISH results reported in Table SII. For each probe, values show the difference between the total number of signals recorded after culture and that of fresh tissue. Data were divided according to loss (number of signals/cell <2), disomy (number of signals/cell =2), and gain (number of signals/cell  $\geq$ 3). HGIN, high grade infiltrating; HGNI, high grade non-infiltrating; LGIN, low grade infiltrating; LGNI, low grade non-infiltrating.

Please note: Wiley-Blackwell are not responsible for the content or functionality of any supporting materials supplied by the authors. Any queries (other than missing material) should be directed to the corresponding author for the article.